

## Analysis of $\pi d$ elastic scattering data to 500 MeV

Richard A. Arndt, Igor I. Strakovsky\* and Ron L. Workman

*Department of Physics, Virginia Polytechnic Institute and State University, Blacksburg, Virginia 24061*

(Received 19 May 1994)

An energy-dependent and a set of single-energy partial-wave analyses of  $\pi d$  elastic scattering data have been completed. Amplitudes are presented for pion laboratory kinetic energies up to 500 MeV. These results are compared with those found in other recent analyses. We comment on the present database and make suggestions for future work.

PACS number(s): 11.80.Et, 14.20.Pt, 25.40.Ep, 25.80.Hp

### I. INTRODUCTION

The  $\pi d$  system is an important component of the more general  $\pi NN$  problem. At intermediate energies, the  $\pi d$  and  $N\Delta$  channels provide much of the inelasticity associated with  $pp$  scattering [1]. We have previously analyzed the  $pp \rightarrow pp$  [2] and  $\pi d \rightarrow pp$  [3] reactions. Here we give the results of our analyses of  $\pi d$  elastic scattering data.

A number of calculations have resulted in a reasonable qualitative (and over some regions quantitative) description of  $\pi d$  scattering data [1]. The more theoretical approaches have had difficulty in describing all observables [1], and have generally concentrated on limited kinematic regions. In addition, several partial-wave [4–8] analyses have been performed. These analyses have found some motivation from claims [9] of dibaryon resonances in  $pp$  and  $\pi d \rightarrow pp$  scattering reactions. Comparisons with data have been complicated by the occasional appearance and subsequent disappearance of sharp structures in some polarization observables. We plan to examine these questions through a coupled-channel analysis of  $pp$  and  $\pi d$  elastic scattering combined with  $\pi d \rightarrow pp$ . However, as a first step, we have analyzed  $\pi d$  elastic scattering separately.

The present analyses include measurements to 500 MeV in the laboratory kinetic energy of the pion. (This corresponds to laboratory kinetic energies between 287.5 MeV and 1287 MeV in the  $pp$  system.) The value of  $\sqrt{s}$  varies from 2.015 GeV to 2.437 GeV, and spans the range of energies typically associated with dibaryon candidates. This reaction displays the same “resonance-like” behavior found in partial-wave analyses of  $pp \rightarrow pp$  and  $\pi d \rightarrow pp$  scattering data. The interpretation of this behavior generally arouses strong reactions, either for or against the existence of intermediate dibaryon resonances. In the present work, our goal is simply a refined understanding of the  $\pi d$  elastic scattering amplitudes. Interpretations will depend upon the results of our larger joint analysis of the  $pp$  and  $\pi d$  channels.

In the next section, we will make some comments on

the database used in this analysis. In Sec. III, we will outline the general formalism for  $\pi d$  elastic scattering. Methods used in the partial-wave analysis will be discussed in Sec. IV. Our main results will be presented in Sec. V. Here we will also compare with the available data and other recent analyses. Finally, in Sec. VI, we will summarize our findings and make some suggestions for future investigations.

### II. DATABASE

Experimental studies of  $\pi d$  elastic scattering began to produce results in the 1950s. At this time, the first measurements of total and differential cross sections became available. The trend of  $\pi d$  elastic scattering data accumulation since 1952 is displayed in Fig. 1. The rapid increase in the number and type of measurements in the early 1980s was motivated by a growing interest in the problem of exotics. This reaction was expected to give further information on the existence (or nonexistence) of dibaryon states suggested in analyses of  $NN$  elastic scattering data. Numerous high-quality deuteron polarization measurements were made. The total database more than doubled, and several partial-wave analyses [4–8] were carried out at this time. The present study has utilized a set of data which is significantly larger, and covers a broader energy interval.

Our total set of experimental data [10–57] (1362 points) includes measurements of the  $\pi^+d$  (57) and  $\pi^-d$  (67) total cross sections ( $\sigma_T$ ),  $\pi^+d$  (516) and  $\pi^-d$  (236) differential cross sections ( $d\sigma/d\Omega$ ) with unpolarized targets, the deuteron vector analyzing power ( $iT_{11}$ ) for  $\pi^+d$  (280) and  $\pi^-d$  (5), the deuteron tensor analyzing power ( $T_{20}$ ) for  $\pi^+d$  (42), the combined deuteron tensor analyzing powers ( $\tau_{21}$  and  $\tau_{22}$ ) for  $\pi^+d$  (123), and the laboratory deuteron tensor analyzing power ( $t_{20}^{\text{lab}}$ ) for  $\pi^+d$  (30). We have also included 6 unpolarized total elastic cross sections ( $\sigma_T^{\text{el}}$ ). Energy-angle distributions for  $d\sigma/d\Omega$ ,  $iT_{11}$ , and  $T_{20}$  are given in Fig. 2. Most of the  $\pi^+d$  data are concentrated at low energies; the  $\pi^-d$  data tend to span a wider energy range.

As shown in Table I, we have removed  $\sigma_T$  (2),  $d\sigma/d\Omega$  (88),  $\sigma_T^{\text{el}}$  (3),  $iT_{11}$  (6), and  $t_{20}^{\text{lab}}$  (35) data corresponding

---

\*On leave from St. Petersburg Nuclear Physics Institute, Gatchina, St. Petersburg, 188350 Russia.

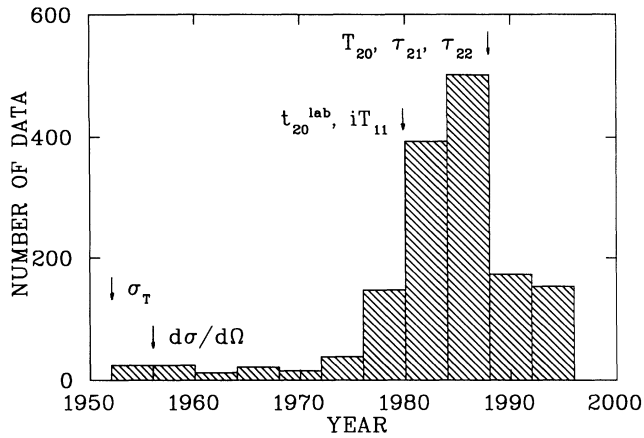


FIG. 1. Data accumulation from 1952 to the present. Arrows indicate the year when measurements of particular observables were first published.

to 9% of the total. These measurements were the source of serious conflicts within the database and were not included in the analysis. For instance, many of the  $t_{20}^{lab}$  measurements (33 points) were produced by the Zürich group [32]. These were found to be in conflict with a number of independent measurements at LAMPF [27,28,56], TRIUMF [52,54], and PSI [44].

### III. FORMALISM

The relations between partial-wave amplitudes and observables have been given in a number of previous theoretical and phenomenological studies. Many of these relations are given in the work of Grein and Locher [58]. They have been included here for completeness and to define our notation. Due to parity conservation, there are

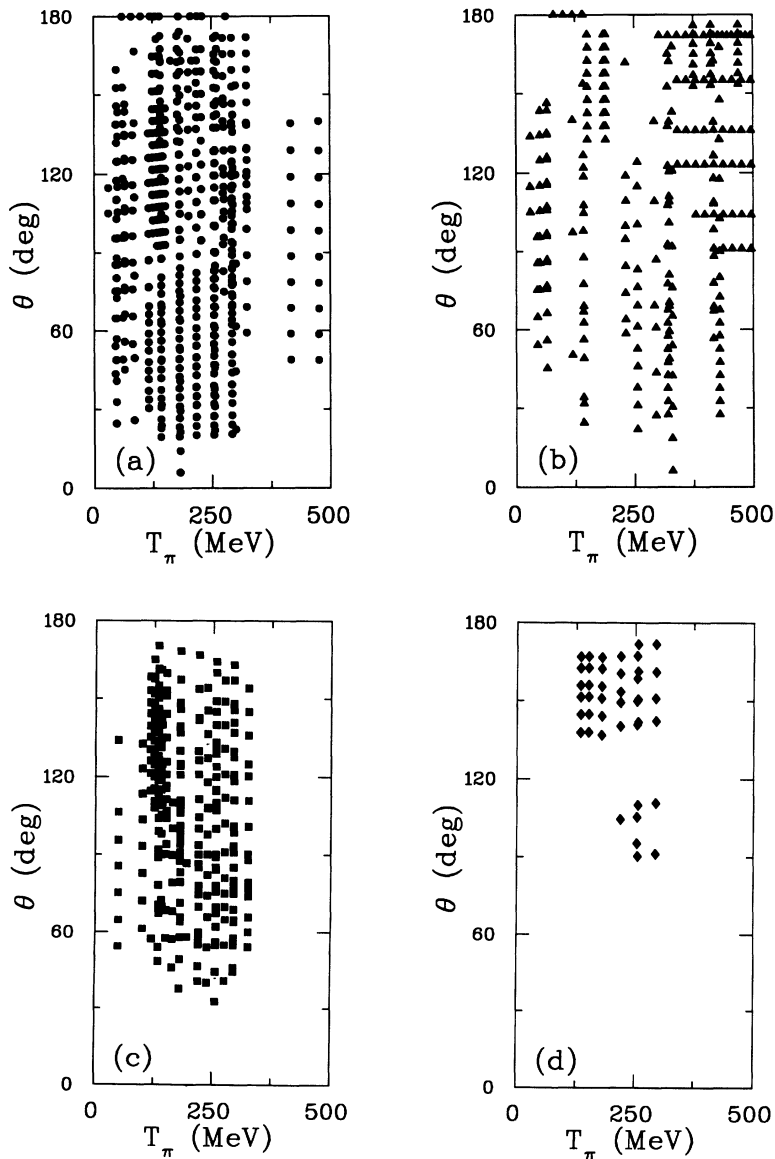


FIG. 2. Energy-angle distribution of total data set. (a) Differential cross section  $d\sigma/d\Omega$  for  $\pi^+d$ , (b) differential cross section  $d\sigma/d\Omega$  for  $\pi^-d$ , (c) deuteron vector analyzing power  $iT_{11}$  for  $\pi^+d$ , and (d) deuteron tensor analyzing power  $T_{20}$  for  $\pi^+d$ .

TABLE I. Number and type of observables used in the present analysis to 500 MeV in the pion laboratory kinetic energy. The number of excluded data is also given.

Observable	$\pi^+ d$		$\pi^- d$	
	No. of data	Deleted data	No. of data	Deleted data
$\sigma_T$	57	0	69	2 <sup>a</sup>
$d\sigma/d\Omega$	572	56 <sup>b</sup>	268	32 <sup>c</sup>
$\sigma_T^{\text{el}}$	3	0	6	3 <sup>d</sup>
$iT_{11}$	285	5 <sup>e</sup>	6	1 <sup>f</sup>
$T_{20}$	42	0	0	0
$\tau_{21}$	47	0	0	0
$\tau_{22}$	76	0	0	0
$t_{20}^{\text{lab}}$	65	35 <sup>g</sup>	0	0
Total	1147	96	349	38
No. of energies	239	16	121	11

<sup>a</sup>See Refs. [19] and [29].

<sup>b</sup>See Refs. [25], [40], [34], and [39].

<sup>c</sup>See Refs. [10], [19], [39], and [41].

<sup>d</sup>See Refs. [19], [41], and [46].

<sup>e</sup>See Ref. [51].

<sup>f</sup>See Ref. [35].

<sup>g</sup>See Refs. [32] and [54].

four independent helicity amplitudes for this reaction. Thus, for a reconstruction of the scattering amplitude at fixed values of the energy and scattering angle, one requires seven independent measurements. The amplitude

$H_{\alpha\beta}(\theta)$  is labeled by the deuteron helicities ( $\alpha$  and  $\beta$ ) in initial and final states. Here the angle  $\theta$  is the center-of-mass scattering angle of the outgoing pion. Our notation for the helicity amplitudes [58] is given below:

$$\begin{aligned}
 H_{++} \equiv H_1 &= \frac{1}{2} \sum_{J \geq 1} [(J+1) T_{J-1}^J J_{-1} + J T_{J+1}^J J_{+1} + (2J+1) T_J^J J + 2 \sqrt{J(J+1)} T_{J-1}^J J_{+1}] d_{11}^J, \\
 H_{+0} \equiv H_2 &= -\frac{1}{2} \sum_{J \geq 1} [\sqrt{2(J+1)} (T_{J+1}^J J_{+1} - T_{J-1}^J J_{-1}) + \sqrt{2} T_{J-1}^J J_{+1}] d_{10}^J, \\
 H_{+-} \equiv H_3 &= \frac{1}{2} \sum_{J \geq 1} [(J+1) T_{J-1}^J J_{-1} + J T_{J+1}^J J_{+1} - (2J+1) T_J^J J + 2 \sqrt{J(J+1)} T_{J-1}^J J_{+1}] d_{1-1}^J, \\
 H_{00} \equiv H_4 &= \sum_{J \geq 0} [J T_{J-1}^J J_{-1} + (J+1) T_{J+1}^J J_{+1} - 2\sqrt{J(J+1)} T_{J-1}^J J_{+1}] d_{00}^J,
 \end{aligned} \tag{1}$$

where the  $d_{\alpha\beta}^J$  are reduced rotation matrices. The symmetry relations

$$\begin{aligned}
 H_{\alpha\beta} &= (-1)^{\alpha+\beta} H_{-\alpha-\beta}, \\
 H_{0\beta} &= -H_{\beta 0}
 \end{aligned} \tag{2}$$

are also obeyed by the above helicity amplitudes. The partial-wave amplitudes  $T_{L\pi', L\pi}^J$  are labeled by the values of  $L\pi'$  corresponding to the  $\pi d$  final state, and  $L\pi$  for the  $\pi d$  initial state. In the next section, and in our figures, we use the notation  ${}^3L_J^\pi$ , and  $\epsilon_J$  for the amplitudes  ${}^3(J-1)_J - {}^3(J+1)_J$  as in Ref. [2].

The various observables for  $\pi d$  elastic scattering are given in terms of helicity amplitudes [58,59] below:

$$\begin{aligned}
 I_0 &\equiv t_{00}^{00} = 2 |H_1|^2 + 4 |H_2|^2 + 2 |H_3|^2 + |H_4|^2, \\
 \frac{d\sigma}{d\Omega} &= \sigma_g I_0, \\
 \sigma_T^{\text{el}} &= 4\pi\sigma_g \int_0^\pi I_0 \sin\theta d\theta,
 \end{aligned} \tag{3}$$

$$\begin{aligned}
 \sigma_T &= 4\pi\sigma_g [2\text{Im}H_1(0) + \text{Im}H_4(0)], \\
 \sigma_T^{\text{aligned}} &= 8\pi\sigma_g [\text{Im}H_1(0) - \text{Im}H_4(0)], \\
 iT_{11} &\equiv it_{11}^{00} = -\sqrt{6} \text{Im}[H_2^*(H_1 - H_3 + H_4)]/I_0, \\
 T_{20} &\equiv t_{20}^{00} = \sqrt{2} (|H_1|^2 - |H_2|^2 + |H_3|^2 - |H_4|^2)/I_0, \\
 T_{21} &\equiv -t_{21}^{00} = -\sqrt{6} \text{Re}[H_2^*(H_1 - H_3 - H_4)]/I_0, \\
 T_{22} &\equiv t_{22}^{00} = \sqrt{3} [2 \text{Re}(H_1^* H_3) - |H_2|^2]/I_0, \\
 t_{10}^{10} &= 3 (|H_1|^2 - |H_3|^2)/I_0, \\
 t_{11}^{10} &= 3 \text{Re}[H_2^*(H_1 + H_3)]/I_0, \\
 it_{21}^{10} &= 3 \text{Im}[H_2^*(H_1 + H_3)]/I_0, \\
 it_{22}^{10} &= 3 \sqrt{2} \text{Im}(H_1^* H_3)/I_0, \\
 t_{11}^{11} &= 3 [\text{Re}(H_1^* H_4) + |H_2|^2]/I_0, \\
 t_{1-1}^{11} &= 3 [-\text{Re}(H_3^* H_4) + |H_2|^2]/I_0, \\
 it_{20}^{11} &= -\sqrt{3} \text{Im}[H_2^*(H_1 - H_3 - 2H_4)]/I_0, \\
 it_{21}^{11} &= -3 \text{Im}(H_1^* H_4)/I_0, \\
 it_{2-1}^{11} &= -3 \text{Im}(H_3^* H_4)/I_0,
 \end{aligned}$$

$$\begin{aligned}
t_{22}^{11} &= 3 \sqrt{2} \operatorname{Im}(H_2^* H_1)/I_0, \\
t_{2-2}^{11} &= -3 \sqrt{2} \operatorname{Im}(H_2^* H_3)/I_0, \\
t_{20}^{20} &= (|H_1|^2 - 4 |H_2|^2 + |H_3|^2 - 2 |H_4|^2)/I_0, \\
t_{21}^{20} &= \sqrt{3} \operatorname{Re}[H_2^*(H_1 - H_3 + 2 H_4)]/I_0, \\
t_{22}^{20} &= \sqrt{6} [\operatorname{Re}(H_1^* H_3) + |H_2|^2]/I_0, \\
t_{21}^{21} &= 3 [\operatorname{Re}(H_1^* H_4) - |H_2|^2]/I_0, \\
t_{2-1}^{21} &= 3 [\operatorname{Re}(H_3^* H_4) + |H_2|^2]/I_0, \\
t_{22}^{21} &= 3 \sqrt{2} \operatorname{Re}(H_2^* H_1)/I_0, \\
t_{2-2}^{21} &= -3 \sqrt{2} \operatorname{Re}(H_2^* H_3)/I_0, \\
t_{22}^{22} &= 3 |H_1|^2/I_0, \\
t_{2-2}^{22} &= 3 |H_3|^2/I_0.
\end{aligned}$$

In these relations the factor  $\sigma_g$  is equal to  $\frac{1}{3} \left(\frac{k}{k_\pi}\right)^2$ , where  $k_\pi$  is pion momentum in the center-of-mass frame. Here the  $t$ 's are spherical harmonics [60]. The asterisk denotes complex conjugation. We have followed the Madison convention [58] in defining a coordinate system. The

observables  $d\sigma/d\Omega$ ,  $\sigma_T^{\text{el}}$ , and  $\sigma_T$  are the usual unpolarized cross sections.  $\sigma_T^{\text{aligned}}$  gives the spin-aligned total cross section. The other observables involve either the polarization of the initial or final deuteron ( $iT_{11}$ ,  $T_{20}$ ,  $T_{21}$ , and  $T_{22}$ ) or both. The following relationships are valid due to parity conservation and time reversal invariance:

$$\begin{aligned}
t_{L'M'}^{LM} &= (-1)^{L+L'+M+M'} t_{L'-M'}^{L-M}, \\
t_{L'M'}^{LM} &= (-1)^{M+M'} t_{LM'}^{L'M}.
\end{aligned} \tag{4}$$

We also require some combinations of deuteron tensor analyzing powers measured by experimentalists. In Ref. [45],  $\tau_{21}$  and  $\tau_{22}$  are defined by

$$\begin{aligned}
\tau_{22} &= \sqrt{\frac{1}{6}} T_{20} + T_{22}, \\
\tau_{21} &= T_{21} + \frac{1}{2} \tau_{22} = \frac{1}{2} \sqrt{\frac{1}{6}} T_{20} + T_{21} + \frac{1}{2} T_{22}.
\end{aligned} \tag{5}$$

The laboratory deuteron tensor analyzing powers expressed [45] in terms of c.m. variables are

$$\begin{aligned}
t_{20}^{\text{lab}} &= \frac{3 \cos^2 \theta_R - 1}{2} T_{20} + 2 \sqrt{\frac{3}{2}} \sin \theta_R \cos \theta_R T_{21} + \frac{3}{2} \sin^2 \theta_R T_{22}, \\
t_{21}^{\text{lab}} &= \sqrt{\frac{3}{2}} \sin \theta_R \cos \theta_R T_{20} + (1 - 2 \cos^2 \theta_R) T_{21} - \sin \theta_R \cos \theta_R T_{22}, \\
t_{22}^{\text{lab}} &= \frac{1}{2} \sqrt{\frac{3}{2}} \sin^2 \theta_R T_{20} - \sin \theta_R \cos \theta_R T_{21} + \frac{1 + \cos^2 \theta_R}{2} T_{22},
\end{aligned} \tag{6}$$

where  $\theta_R$  is the deuteron recoil angle in the laboratory frame.

#### IV. PARTIAL-WAVE ANALYSIS

The energy dependence of our global fit was obtained through a coupled-channel  $K$ -matrix form, in order to ensure that unitarity would not be violated. The “inelastic” channel was nonspecific but included to account for the coupled  $pp$  and  $N\Delta$  reactions. For single-channel  $\pi d$  states (for example,  ${}^3D_2$ ) this resulted in a  $2 \times 2$  matrix, and for the spin-coupled states (for example,  ${}^3P_2$ ,  $\epsilon_2$ ,  ${}^3F_2$ ) we had a  $3 \times 3$  matrix. The matrix elements were expanded as polynomials in the pion laboratory energy, and an appropriate phase-space factor was included in the  $\pi d$  elastic elements to ensure proper threshold behavior. This analysis included 21 searched partial waves and 66 varied parameters. Amplitudes with  $J \leq 5$  were considered. The solution gave a  $\chi^2$  of 2743 for the 1362 data and 333 experiments below 500 MeV. Coulomb modifications of the phase-space factors were attempted but discarded in the final fit; the sensitivity to such refinements appeared minimal.

Single-energy solutions were produced up to 300 MeV, using a binning width of  $10 \pm 5$  MeV. We used mainly the

energy values chosen in previous single-energy partial-wave analyses [4–7]. Starting values for the partial-wave amplitudes, as well as their (fixed) energy derivatives, were obtained from the energy-dependent fit. The scattering database was supplemented with a constraint on each varied amplitude. Constraint errors were taken to be 0.02. This was added, in quadrature, to 5% of the amplitude. Such constraints were essential to prevent the solutions from “running away” when the bin was relatively empty of scattering data. These errors were generous enough that they afforded little constraint for those solutions where sufficient data existed within the bin.

Single-energy analyses are done in order to reveal “structure” which may be missing from the energy-dependent fit. Little compelling evidence was found for such structure. Results of the single-energy analyses are summarized in Table II. A maximum of nine partial waves ( ${}^3S_1$ ,  $\epsilon_1$ ,  ${}^3P_{0,1,2}$ ,  ${}^3D_{2,3}$ , and  ${}^3F_{3,4}$ ) were searched in the single-energy analyses. The remaining partial waves were fixed at the energy-dependent values.

Several Coulomb correction schemes were tested. Our results were found to be relatively independent of the chosen form. Differences are most apparent in charge-asymmetry observables, as shown in Ref. [61]. In the present analysis, we have adopted Hiroshige’s formulation [8].

TABLE II. Single-energy (binned) fits and  $\chi^2$  values.  $N_{\text{prm}}$  is the number of amplitudes (real + imaginary) varied in the fit.  $\chi_C^2$  is due to the amplitude constraints,  $\chi_D^2$  is the contribution from data, and  $\chi_E^2$  is given by the energy-dependent fit SM94.

$T_\pi$ (MeV)	Range (MeV)	$N_{\text{data}}$	$N_{\text{prm}}$	$\chi_C^2$	$\chi_D^2$	$\chi_E^2$
65	58.0–72.0	54	4	2.4	86.6	129.9
87	72.0–85.5	24	8	0.4	20.4	30.3
111	107.5–125.2	82	8	0.7	68.9	68.9
125	115.0–134.0	170	12	5.1	154.1	205.0
134	124.0–142.8	258	12	4.2	293.6	362.1
142	133.0–152.0	284	14	8.1	345.4	442.6
151	141.0–160.6	154	16	11.0	186.9	256.3
182	174.0–189.5	168	16	19.6	300.3	445.8
216	206.0–220.0	99	18	1.6	121.3	148.1
230	220.0–238.0	53	18	7.8	51.3	96.5
256	254.0–260.0	125	18	2.9	132.5	200.6
275	270.5–284.4	40	18	2.9	17.4	42.6
294	284.4–300.0	132	16	3.3	228.5	263.6

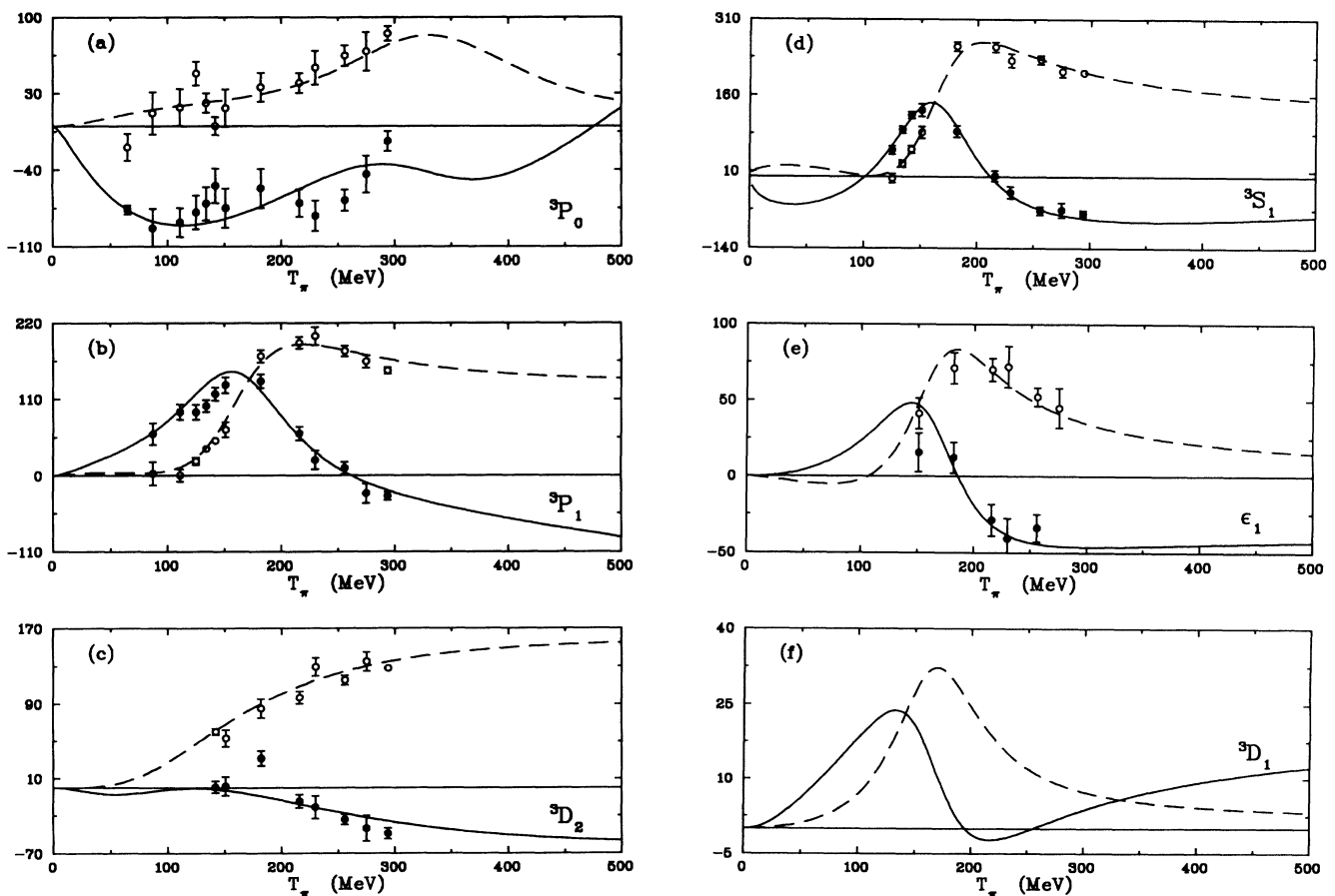


FIG. 3. Partial-wave amplitudes from 0 to 500 MeV. Solid curves are the real parts of amplitudes; dashed curves are the imaginary parts. Single-energy solutions are plotted as solid circles (real part) and open circles (imaginary part). All amplitudes have been multiplied by a factor of  $10^3$ , and are dimensionless.

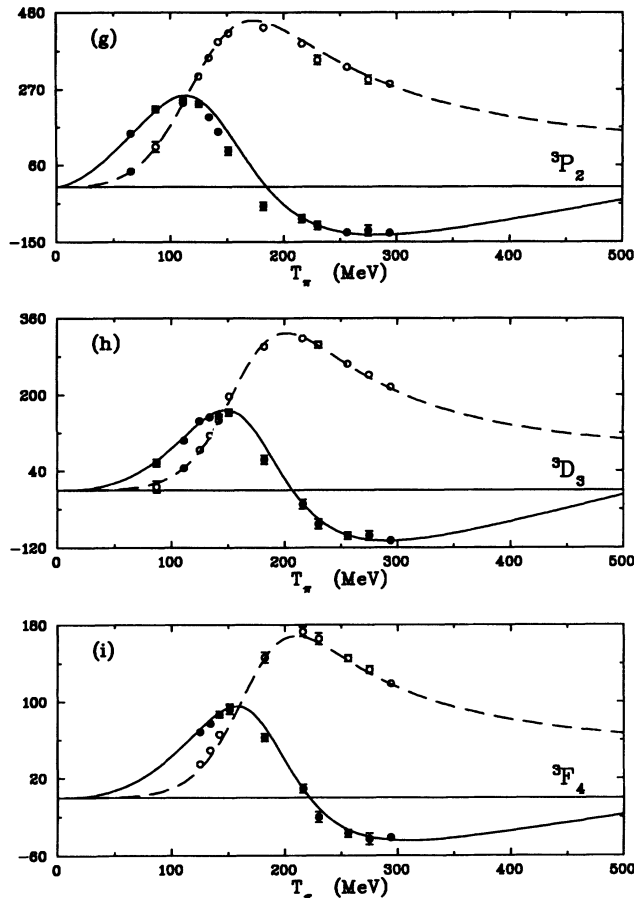


FIG. 3. (Continued).

## V. RESULTS AND COMPARISONS

Results for the partial-wave amplitudes, defined in Eq. (1), are shown in Fig. 3. Over our energy range, the dominant amplitudes are the  ${}^3S_1$ ,  ${}^3P_1$ ,  ${}^3P_2$ ,  ${}^3D_2$ ,  ${}^3D_3$ , and  ${}^3F_4$ . The compatibility of our energy-dependent and single-energy solutions is also evident in Fig. 3. The lack of single-energy solutions beyond 300 MeV is due to the data distribution displayed in Fig. 2.

As mentioned in Sec. IV, the energy-dependent solution gives a reasonable overall fit to the data. While the  $\chi^2/\text{datum}$  was about 2 for the selected database, a much higher value would have resulted from the total set of measurements. Some of the data conflicts are apparent in Fig. 4, where we have given predictions for observables at  $T_{\pi^+} = 256$  MeV. The data are generally well described at this energy, except possibly the most forward  $iT_{11}$  measurements. We should mention that  $\pi^-d$  measurements account for only about a quarter of the total data set. In addition, there is a noticeable difference in the  $\chi^2/\text{datum}$  (1.86 for  $\pi^+d$  versus 2.55 for  $\pi^-d$ ). Various  $\pi^+d$  total cross sections are plotted in Fig. 5.

We have also compared our results to those from several other groups. The last single-energy partial-

wave analyses for  $\pi d$  elastic scattering were published by the Grenoble-Rehovot [4], Osaka [5], Saskatoon [6], and Mexico-Karlsruhe [7] groups. These results have generally covered a more narrow energy interval (seven points from 82 to 292 MeV in [4], eight points from 114 to 325 MeV in [5], nine points from 117 to 324 MeV in [6], and two points at 256 and 294 MeV in [7]). The energy-dependent analysis of Ref. [8] covered the region between 65 MeV and 275 MeV. We have plotted our energy-dependent results along with several analyses in Fig. 6. The figure displays the experimental version of model (iv) from Ref. [7], and the version of Ref. [6] using Blankleider-Afnan [60] model amplitudes as input. The agreement is qualitative at best.

## VI. SUMMARY AND CONCLUSIONS

In this work we have analyzed a  $\pi d$  elastic scattering database which is significantly larger than those used in previously published analyses. A reasonable fit to this database was found. While there are considerable differences between the results of this and previous analyses, one common qualitative feature is present. Several dom-

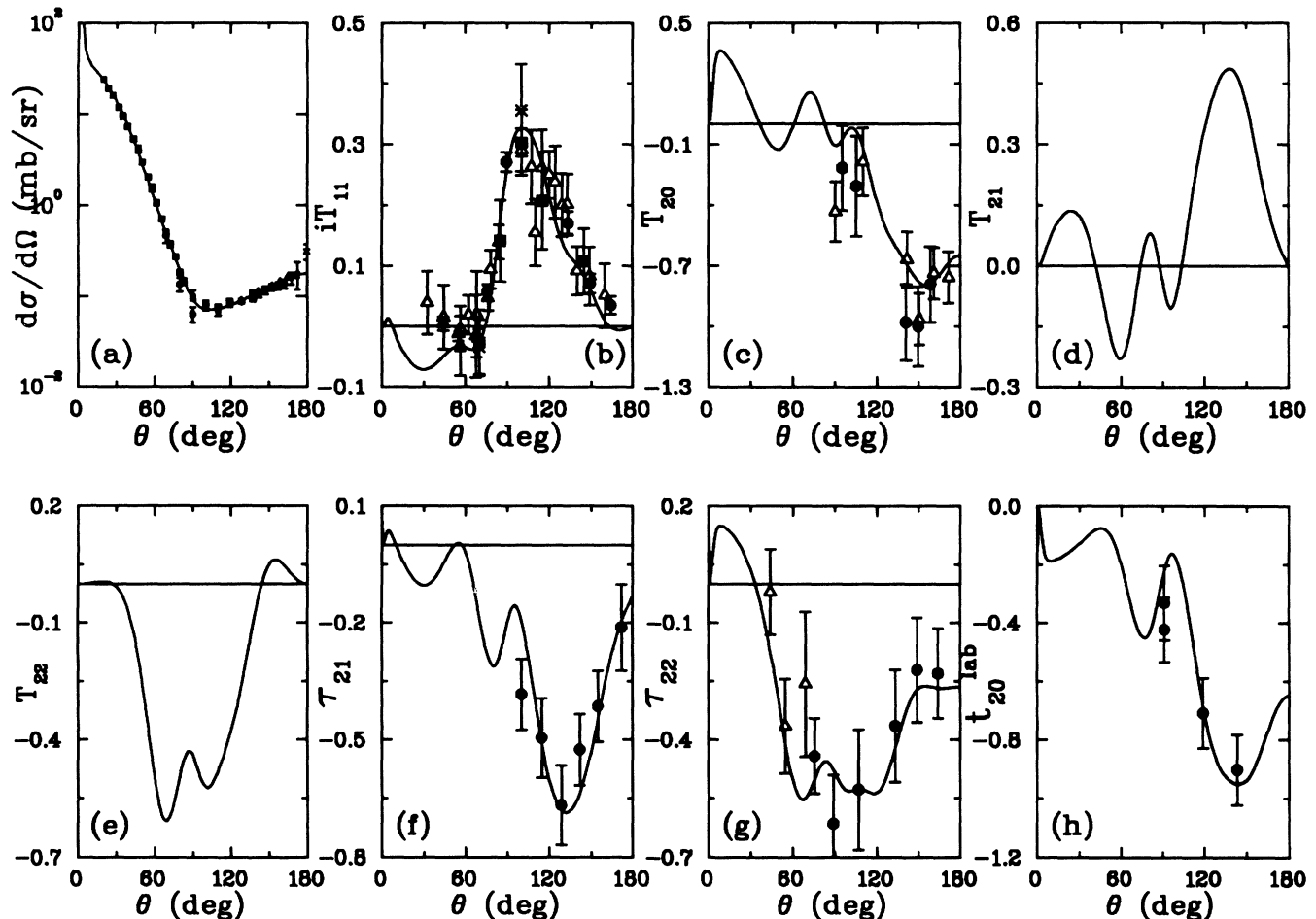


FIG. 4. Predictions for  $\pi^+d$  observables at  $T_\pi = 256$  MeV. Data have been normalized. (a)  $d\sigma/d\Omega$ , (b)  $iT_{11}$ , (c)  $T_{20}$ , (d)  $T_{21}$ , (e)  $T_{22}$ , (f)  $\tau_{21}$ , (g)  $\tau_{22}$ , and (h)  $t_{20}^{\text{lab}}$ .

inant partial-wave amplitudes display a “resonancelike” behavior. The correlation between these amplitudes is particularly evident in the Argand plot of Fig. 7. This behavior is very similar to that found in our recent analyses of  $\pi d \rightarrow pp$  [3] and  $pp$  [2] elastic scattering data.

The present work is completely free of model-based constraints. Previous analyses have generally used theory as a guide where insufficient experimental information was available. This factor is a likely source for some of the discrepancies evident in Fig. 6. The evolving database provides another.

While we have analyzed data to 500 MeV, the results above 300 MeV should not be taken too seriously. Most of the database is concentrated below 300 MeV, with only about 200 measurements covering the region between 300 MeV and 500 MeV. Clearly, we require much additional (and more consistent) data to define a unique solution (both above and below 300 MeV). We should mention that the present solution predicts a rich structure for many of the spin-transfer observables defined in Eqs. (3). While only a few of these quantities have been measured, some new PSI measurements [62] of  $t_{11}^{11}$ ,  $it_{20}^{11}$ ,  $it_{21}^{11}$ , and  $t_{22}^{11}$

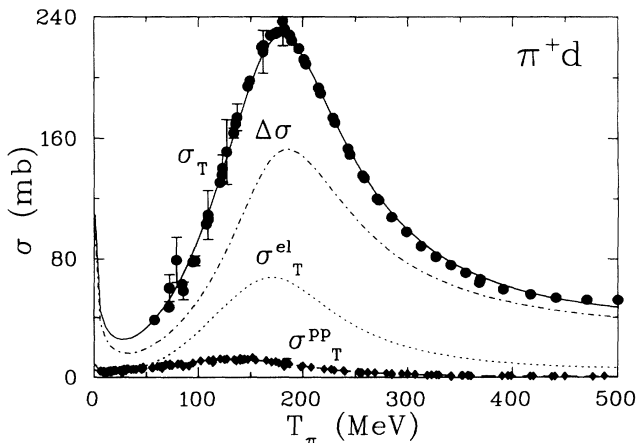


FIG. 5. Total cross sections  $\sigma$  for  $\pi^+d$  scattering. (a) Unpolarized total cross section  $\sigma_T$  (solid curve), (b) contribution [3] from  $\pi^+d \rightarrow pp$   $\sigma_T^{pp}$  (dashed curve), (c) the total elastic cross section  $\sigma_T^{\text{el}}$  (dotted curve), and the remainder  $\Delta\sigma$  given by  $\sigma_T - \sigma_T^{\text{el}} - \sigma_T^{pp}$ .

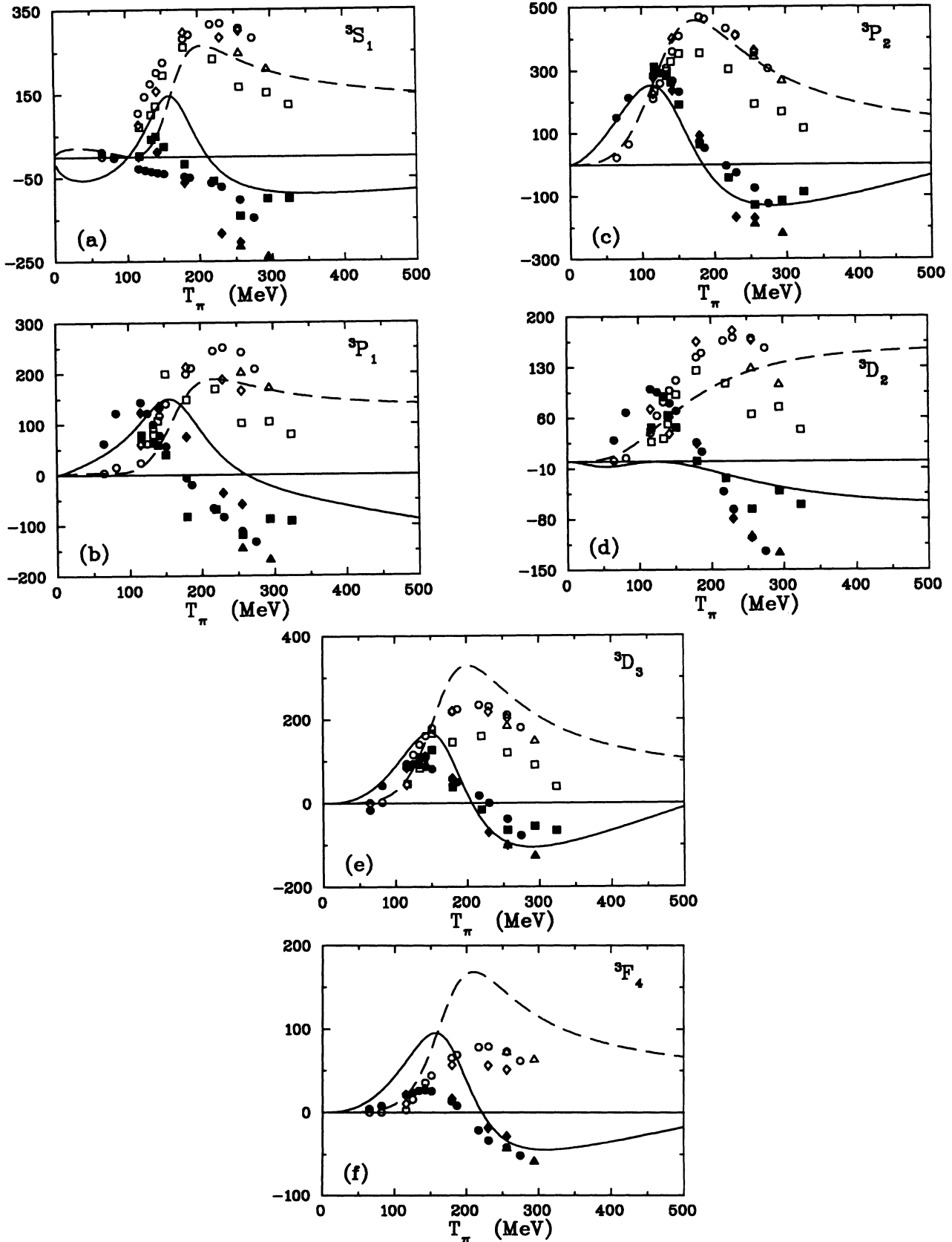


FIG. 6. Plots of the amplitudes (a)  ${}^3S_1$ , (b)  ${}^3P_1$ , (c)  ${}^3P_2$ , (d)  ${}^3D_2$ , (e)  ${}^3D_3$ , and (f)  ${}^3F_4$ . The solid (dashed) curves give the real (imaginary) part from the present energy-dependent solution. The circles, squares, triangles, and diamonds are results from Refs. [8], [6], [7], and [4], respectively. Solid symbols give real parts; open symbols give imaginary parts. All amplitudes have been multiplied by a factor of  $10^3$ , and are dimensionless.



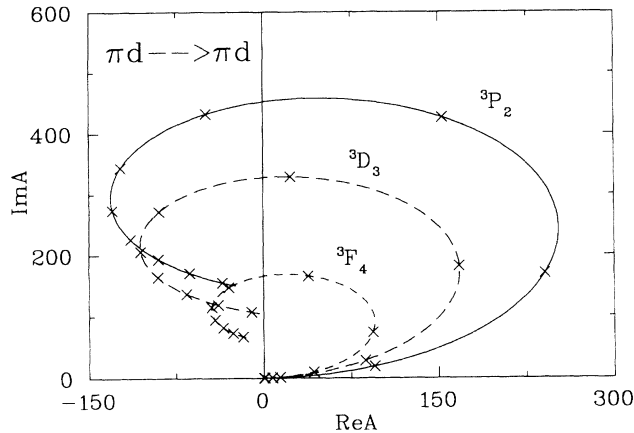


FIG. 7. Argand plot of the dominant  $\pi d$  partial-wave amplitudes  ${}^3P_2$ ,  ${}^3D_3$ , and  ${}^3F_4$  which correspond to the  ${}^1D_2$ ,  ${}^3F_3$ , and  ${}^1G_4$   $pp$  states, respectively. (Compare Fig. 7 of Ref. [3]). The X points denote 50 MeV steps. All amplitudes have been multiplied by a factor of  $10^3$ .

at 134, 180, and 219 MeV will soon be available.

This reaction is now incorporated into the SAID program [63], which is maintained at Virginia Tech. Detailed information regarding the database, partial-wave

amplitudes, and observables may be obtained either interactively, through the SAID system (for those who have access to TELNET), or directly from the authors.

## ACKNOWLEDGMENTS

The authors express their gratitude to J.L. Beveridge, B. Brinkmüller, D.V. Bugg, J.-P. Egger, R.R. Johnson, R. Meier, R.C. Minehart, R.J. Peterson, R.A. Ristinen, B. Saghai, G.R. Smith, N.R. Stevenson, Y. Sumi, and R. Tacik for providing experimental data prior to publication and clarification of information already published. We are grateful to D.V. Bugg, N. Hiroshige, G. Jones, M.P. Locher, D.F. Measday, T. Mizutani, A. Rinat, R.A. Ristinen, and G.R. Smith for providing available partial-wave solutions and for helpful information concerning the various Coulomb correction schemes. I.S. acknowledges the hospitality extended by the Physics Department of Virginia Tech. This work was supported in part by the U.S. Department of Energy Grant No. DE-FG05-88ER40454.

- [1] H. Garcilazo and T. Mizutani,  *$\pi NN$  Systems* (World Scientific, Singapore, 1990). This reference gives a good review of the various theoretical approaches to  $\pi d$  elastic scattering and other  $\pi NN$  problems.
- [2] R.A. Arndt, L.D. Roper, R.L. Workman, and M.W. McNaughton, *Phys. Rev. D* **45**, 3995 (1992).
- [3] R.A. Arndt, I.I. Strakovsky, R.L. Workman, and D.V. Bugg, *Phys. Rev. C* **48**, 1926 (1993); **49**, 1229(E) (1994).
- [4] J. Arvieux and A.S. Rinat, *Nucl. Phys.* **A350**, 205 (1980); J. Arvieux, *Phys. Lett.* **103B**, 99 (1981); A.S. Rinat (private communication).
- [5] N. Hiroshige, W. Watari, and M. Yonezawa, *Prog. Theor. Phys.* **68**, 327 (1982); **72**, 1282 (1984); N. Hiroshige, M. Kawasaki, W. Watari, and M. Yonezawa, *ibid.* **84**, 941 (1990).
- [6] N.R. Stevenson and Y.M. Shin, *Phys. Rev. C* **36**, 1221 (1987).
- [7] H. Garcilazo, E.T. Boschitz, W. Gyles, W. List, C.R. Otterman, R. Tacik, and M. Wessler, *Phys. Rev. C* **39**, 942 (1989).
- [8] N. Hiroshige (private communication).
- [9] See, for example, A. Yokosawa, in *High Energy Spin Physics (Conference Report)*, Proceedings of 9th International Symposium on High Energy Spin Physics, Bonn, Germany, 1990, edited by K.-H. Althoff and W. Meyer (Springer-Verlag, Berlin, 1991), Vol. 1, p. 526; I.I. Strakovsky, *Fiz. Elem. Chastits At. Yadra* **22**, 615 (1991) [*Sov. J. Nucl. Part.* **22**, 296 (1991)], and references therein.
- [10] M. Akemoto, K. Baba, I. Endo, H. Himemiya, K. Inoue, T. Kawamoto, Y. Maeda, T. Ohsugi, R. Ohtani, Y. Sumi, T. Takeshita, S. Uehara, T. Umeda, and T. Maki, *Phys. Rev. Lett.* **50**, 400 (1983); M. Akemoto, K. Baba, I. Endo, H. Himemiya, K. Inoue, T. Kawamoto, Y. Maeda, T. Ohsugi, R. Ohtani, Y. Sumi, T. Takeshita, S. Uehara, T. Umeda, and T. Maki, *Phys. Rev. Lett.* **51**, 1838 (1983); Y. Sumi (private communication). Deleted 303 MeV and 486 MeV  $d\sigma/d\Omega$  points for  $\pi^- d$  at  $172^\circ$  in this analysis.
- [11] H.L. Anderson, E. Fermi, D.E. Nagle, and G.D. Yodh, *Phys. Rev.* **86**, 413 (1952).
- [12] J. Ashkin, J.P. Blaser, F. Feiner, J.G. Gorman, and M.O. Stern, *Phys. Rev.* **96**, 1104 (1954).
- [13] D. Axen, G. Duesdieker, L. Felawka, Q. Ingram, R. Johnson, G. Jones, D. Lapatourel, M. Salomon, W. Westlund, and L. Robertson, *Nucl. Phys.* **A256**, 387 (1976).
- [14] B. Balestri, P.Y. Bertin, B. Coupat, G. Fournier, A. Gerard, L. Guechi, E.W.A. Ligemann, J. Miller, J. Morgenstern, J. Picard, B. Saghai, K.K. Seth, C. Tzara, and P. Vernin, in *Meson-Nuclear Physics—1979 (Houston)*, Proceedings of the 2nd International Topical Conference on Meson-Nuclear Physics, edited by E.V. Hungerford, AIP Conf. Proc. No. 54 (AIP, New York, 1979), p. 515; B. Balestri, G. Fournier, A. Gerard, J. Miller, J. Morgenstern, J. Picard, B. Saghai, P. Vernin, P.Y. Bertin, B. Coupat, E.W.A. Ligemann, and K.K. Seth, *Nucl. Phys.* **A392**, 217 (1983).
- [15] B. Balestri, G. Fournier, A. Gerard, J. Miller, J. Morgenstern, J. Picard, B. Saghai, P. Vernin, P.Y. Bertin, B. Coupat, E.W.A. Ligemann, and K.K. Seth, *Nucl. Phys.* **A392**, 217 (1983).
- [16] D. Bodansky and A.M. Sachs, *Phys. Rev.* **98**, 240 (1955).
- [17] J. Bolger, E. Boschitz, G. Proebstle, G.R. Smith, S. Mango, F. Volger, R.R. Johnson, and J. Arvieux, *Phys. Rev. Lett.* **46**, 167 (1981); G.R. Smith, E.L. Mathie, E.T. Boschitz, C.R. Otterman, S. Mango, J.A. Konter, M.

- Daum, M. Meyer, R. Olszewski, and F. Vogler, Phys. Rev. C **29**, 2206 (1984).
- [18] J. Bolger, E. Boschitz, E.L. Mathie, G.R. Smith, M. Meyer, F. Volger, S. Mango, J.A. Konter, G.S. Mutchler, and J. Arvieux, Phys. Rev. Lett. **48**, 1667 (1982); G.R. Smith, E.L. Mathie, E.T. Boschitz, C.R. Ottermann, S. Mango, J.A. Konter, M. Daum, M. Meyer, R. Olszewski, and F. Vogler, Phys. Rev. C **29**, 2206 (1984).
- [19] G. Brunhart, G.S. Faughn, and V.P. Kenney, Nuovo Cimento **29**, 1162 (1963). Deleted in this analysis.
- [20] A.A. Carter, K.F. Riley, R.J. Tapper, D.V. Bugg, R.S. Gilmore, K.M. Knight, D.C. Salter, G.H. Stafford, E.J.N. Wilson, J.D. Davies, J.D. Dowell, P.M. Hattersley, R.J. Hommer, and A.W. O'Dell, Phys. Rev. **168**, 1457 (1968); D.V. Bugg (private communication).
- [21] R.H. Cole, J.S. McCarthy, R.C. Minehart, and E.A. Wadlinger, Phys. Rev. C **17**, 681 (1978).
- [22] L.G. Dakhno, A.V. Kravtsov, M.M. Makarov, V.I. Medvedev, G.Z. Obrant, V.I. Poromov, V.V. Sarantsev, G.L. Sokolov, and S.G. Sherman, Yad. Fiz. **31**, 626 (1980) [Sov. J. Nucl. Phys. **31**, 326 (1980)].
- [23] L.S. Dulkova, I.B. Sokolova, and M.G. Shafranov, Zh. Eksp. Teor. Fiz. **35**, 313 (1958) [Sov. Phys. JETP **8**, 217 (1959)].
- [24] R. Frascaria, I. Brissaud, J.P. Didelez, C. Perrin, J.L. Beveridge, J.P. Egger, F. Goetz, P. Gretillat, R.R. Johnson, C. Lunke, E. Schwarz, and B.M. Freedom, Phys. Lett. **91B**, 345 (1980).
- [25] K. Gabathuler, C.R. Cox, J.J. Domingo, J. Rohlin, N.W. Tanner, and C. Wilkin, Nucl. Phys. **B55**, 397 (1973). Deleted nine  $d\sigma/d\Omega$  points for  $\pi^+d$  at 141 MeV, 163 MeV, and 256 MeV in this analysis.
- [26] K. Gabathuler, J. Domingo, P. Gram, W. Hirt, G. Jones, P. Schwaller, J. Zichy, J. Bolger, Q. Ingram, J.P. Albanese, and J. Arveux, Nucl. Phys. **A350**, 253 (1980).
- [27] R.J. Holt, J.R. Specht, E.J. Stephenson, B. Zeidman, R.L. Burman, J.S. Frank, M.J. Leith, J.D. Moses, M.A. Yates-Williams, R.M. Laszewski, and R.P. Redwine, Phys. Rev. Lett. **43**, 1229 (1979); E. Ungricht, W.S. Freeman, D.F. Geesaman, R.J. Holt, J.R. Specht, B. Zeidman, E.J. Stephenson, J.D. Moses, M. Farkhondeh, S. Gilad, and R.P. Redwine, Phys. Rev. C **31**, 934 (1985).
- [28] R.J. Holt, J.R. Specht, K. Stephenson, B. Zeidman, J.S. Frank, M.J. Leith, J.D. Moses, E.J. Stephenson, and R.M. Laszewski, Phys. Rev. Lett. **47**, 472 (1981).
- [29] A.E. Ignatenko, A.I. Mukhin, E.B. Azerov, and B.M. Pontecorvo, Dokl. Akad. Nauk SSSR **103**, 209 (1955). Deleted in this analysis.
- [30] P.J. Isaacs, A.M. Sachs, and J. Steinberger, Phys. Rev. **85**, 803 (1952).
- [31] R. Keller, D.G. Crabb, J.R. O'Fallon, T.J. Richards, L.S. Schroeder, R.J. Ott, J. Trischuk, and J. Va'vra, Phys. Rev. D **11**, 2389 (1975).
- [32] V. König, A. Chisholm, W. Gruebler, J. Ulbricht, P.A. Schmelzbach, M. Merdzan, and K. Elsener, J. Phys. G **9**, L211 (1983). Deleted in this analysis.
- [33] M.D. Kohler, J.T. Brack, B. Clausen, J.J. Kraushaar, B.J. Kriss, R.A. Ristinen, K. Vaziri, G.R. Smith, D.F. Ottewell, M.E. Sevier, R.P. Trelle, and N.R. Stevenson, Phys. Rev. C **44**, 15 (1991).
- [34] M.D. Kohler, R.A. Ristinen, J.J. Kraushaar, B.J. Kriss, E.F. Gibson, G.R. Smith, D.F. Ottewell, J.T. Brack, M. Kermani, J. Jaki, and M. Metzler, Phys. Rev. C **48**, 1884 (1993). Deleted two  $d\sigma/d\Omega$  points for  $\pi^+d$  at 30 MeV in this analysis.
- [35] M. Kohler, B.E. King, N.R. Stevenson, R.R. Schubank, Y.M. Shin, R.A. Ristinen, P. Amaudruz, P.P.J. Delheij, D.C. Healey, B.K. Jennings, D.F. Ottewell, G. Sheffer, G.R. Smith, G.D. Wait, J.T. Brack, A. Feltham, M. Hanna, R.R. Johnson, F.M. Rozon, V. Sossi, D. Vetterli, P. Weber, N. Grion, R. Rui, E.L. Mathie, R. Tacik, M. Yeomans, C.A. Gossett, G.J. Wagner, J.M. Lee, and K.S. Chung, Phys. Rev. C **49**, 1715 (1994). Deleted one  $iT_{11}$  point at  $65^\circ$  and 49 MeV in this analysis.
- [36] A.V. Kravtsov, M.M. Makarov, V.I. Medvedev, G.Z. Obrant, V.I. Poromov, V.V. Sarantsev, G.L. Sokolov, and S.G. Sherman, Nucl. Phys. **A322**, 439 (1979).
- [37] T.G. Masterson, J.J. Kraushaar, R.J. Peterson, R.S. Raymond, R.A. Ristinen, R.L. Boudrie, E.F. Gibson, and A.W. Thomas, Phys. Rev. C **26**, 2091 (1982); R.J. Peterson (private communication).
- [38] E.L. Mathie, G.R. Smith, E. Boschitz, M. Meyer, F. Vogler, M. Daum, S. Mango, and J.A. Konter, Phys. Rev. C **28**, 2558 (1983); C.R. Ottermann, E.T. Boschitz, W. Gyles, W. List, R. Tacik, R.R. Johnson, G.R. Smith, and E.L. Mathie, *ibid.* **32**, 928 (1985).
- [39] T.G. Masterson, J.J. Kraushaar, R.J. Peterson, R.S. Raymond, R.A. Ristinen, J.L. Ulmann, R.L. Boudrie, D.R. Gill, E.F. Gibson, and A.W. Thomas, Phys. Rev. C **30**, 2010 (1984); R.J. Peterson (private communication). Deleted in this analysis.
- [40] R.C. Minehart, J.S. Boswell, J.F. Davis, D. Day, J.S. McCarthy, R.R. Whytney, H.J. Ziock, and E.A. Wadlinger, Phys. Rev. Lett. **46**, 1185 (1981); R.C. Minehart (private communication). Deleted 29  $d\sigma/d\Omega$  points for  $\pi^+d$  at 323 MeV, 417 MeV, and 476 MeV in this analysis.
- [41] D.E. Nagele, Phys. Rev. **97**, 480 (1955). Deleted  $\sigma_T^{\text{el}}$  and  $d\sigma/d\Omega$  in this analysis.
- [42] J.H. Norem, Nucl. Phys. **B33**, 512 (1971); J.H. Norem (private communication).
- [43] C.R. Ottermann, E.T. Boschitz, W. Gyles, W. List, R. Tacik, R.R. Johnson, G.R. Smith, and E.L. Mathie, Phys. Rev. C **32**, 928 (1985).
- [44] C.R. Ottermann, E.T. Boschitz, W. Gyles, W. List R. Tacik, M. Wessler, S. Mango, B. van den Brandt, J.A. Konter, D.R. Gill, and G.R. Gill, Phys. C **38**, 2296 (1988).
- [45] C.R. Ottermann, E.T. Boschitz, H. Garcilazo, W. Gyles, W. List R. Tacik, M. Wessler, S. Mango, B. van den Brandt, J.A. Konter, and E.L. Mathie, Phys. Rev. C **38**, 2310 (1988).
- [46] E.G. Pewitt, T.H. Fields, G.B. Yodh, J.G. Fetkovich, and M. Derrick, Phys. Rev. **131**, 1826 (1963); H.N. Pendleton, *ibid.* **131**, 1833 (1963). Deleted  $\sigma_T^{\text{el}}$  in this analysis.
- [47] E. Pedroni, K. Gabathuler, J.J. Domingo, W. Hirt, P. Schwaller, J. Arvieux, C.H.Q. Ingram, P. Gretillat, J. Piffaretti, N.W. Tanner, and C. Wilkin, Nucl. Phys. **A300**, 321 (1978).
- [48] K.C. Rogers and L.M. Lederman, Phys. Rev. **105**, (1957).
- [49] A.M. Sachs, H. Winick, and B.A. Wooten, Phys. Rev. **109**, 1733 (1958).
- [50] W. Skolnik, Phys. Rev. **98**, 240 (1955).
- [51] G.R. Smith, E.L. Mathie, E.T. Boschitz, C.R. Ottermann, S. Mango, J.A. Konter, M. Daum, M. Meyer, R. Olszewski, and F. Vogler, Phys. Rev. C **29**, 2206 (1984). Deleted five  $iT_{11}$  points for  $\pi^+d$  at 134 MeV and 275 MeV in this analysis.

- [52] G.R. Smith, D.R. Gill, D. Healey, D. Ottewell, G.D. Wait, P. Walden, R.R. Johnson, G. Jones, R. Olszewski, F.M. Rozon, R. Rui, M.E. Sevier, R.P. Trelle, E.L. Mathie, G. Lolos, S.I.H. Naqvi, V. Pafilis, N.R. Stevenson, R.B. Schubank, W. Gyles, C.R. Ottermann, and G.S. Kyle, *Phys. Rev. C* **38**, 251 (1988).
- [53] A. Stanovnik, G. Kernel, N.W. Tanner, T. Bressani, E. Chiavassa, S. Costa, G. Dellacasa, M. Gallio, A. Musso, M. Panighini, K. Bos, E.G. Michaelis, W. van Doesburg, and J.D. Davies, *Phys. Lett.* **94B**, 323 (1980).
- [54] N.R. Stevenson, Y.M. Shin, K. Itoh, G. Retzlaff, D.R. Gill, D.F. Ottewell, G.D. Wait, T.E. Drake, D. Frekers, R.B. Schubank, and G.J. Lolos, *Phys. Rev. C* **39**, 1488 (1989). Deleted 116 MeV and 126 MeV  $t_{20}^{lab}$  points for  $\pi^+d$  at  $150^\circ$  in this analysis.
- [55] R. Tacik, E.T. Boschitz, W. Gyles, M. Wessler, S. Mango, B. van den Brandt, J.A. Konter, D.R. Gill, and P. Weber, *Phys. Rev. C* **42**, 1841 (1990); R. Tacik (private communication).
- [56] E. Ungricht, W.S. Freeman, D.F. Geesaman, R.J. Holt, J.R. Specht, B. Zeidman, E.J. Stephenson, J.D. Moses, M. Farkhondeh, S. Gilad, and R.P. Redwine, *Phys. Rev. C* **31**, 934 (1985).
- [57] M. Wessler *et al.*, *Phys. Rev. C* (submitted); R. Meier (private communication).
- [58] We have used the relations of W. Grein and M.P. Locher [*J. Phys. G* **7**, 1355 (1981)] for the partial-wave and helicity amplitudes. We also use the Madison convention, in *Polarization Phenomena in Nuclear Reactions* (University of Wisconsin Press, Madison, 1971), p. XXV. For some combined deuteron tensor analyzing powers we use the notations of Ref. [45].
- [59] Some relations between observables (which we have verified in this analysis) serve as self-consistency checks. A few useful angle-independent identities are given in Appendix 1 of Ref. [58] [Eq. (A.9) of this reference contains a typographical error]. See also C. Bourrely, E. Leader, and J. Soffer, *Phys. Rep.* **59**, 95 (1980).
- [60] For the spherical harmonics, we use the notation of B. Blankleider and I.R. Afnan, *Phys. Rev. C* **31**, 1380 (1985).
- [61] J. Fröhlich, B. Saghai, C. Fayard, and G.H. Lamot, *Nucl. Phys.* **A435**, 738 (1985).
- [62] B. Brinkmüller (private communication).
- [63] Those with access to TELNET can run the SAID program with a link to VTINTE.PHYS.VT.EDU. The login/password is PHYSICS/QUANTUM. The user may view the current database and compare our solutions to those of other groups.